J Mater Sci: Mater Electron
DOI 10.1007/s10854-016-4783-z

Raman investigation of rutile-phased TiO_2 nanorods/nanoflowers with various reaction times using one step hydrothermal method

M. K. Ahmad[1] · S. M. Mokhtar[1] · C. F. Soon[1] · N. Nafarizal[1] · A. B. Suriani[2] · A. Mohamed[2] · M. H. Mamat[3] · M. F. Malek[3] · M. Shimomura[4] · K. Murakami[4]

Received: 30 December 2015 / Accepted: 4 April 2016

Abstract Rutile-phased titanium dioxide nanorods (r-TNRs) and rutile-phased titanium dioxide nanoflowers (r-TNFs) were deposited on fluorine-doped tin oxide coated glass by using one step hydrothermal method at a fixed temperature of 150 °C. The hydrothermal treatment was conducted by varying the reaction time at 2, 3, 4, 5, 6, 7 and 8 h. The effect of reaction time on surface morphology, structure property, crystallite size and Raman spectra was investigated. The nanostructure samples were analysed using X-ray diffractometer, field emission-scanning electron microscope, micro-Raman spectroscopy, and energy-dispersive X-ray spectroscopy. The resulting micro-Raman spectra show abnormal behaviour of Raman intensity. The micro-Raman spectra of the nanostructure samples exhibit insignificant changes and shifting of Raman bands with increasing reaction time. This behaviour can be attributed to the shape and surface morphology distribution of r-TNRs/r-TNFs.

✉ M. K. Ahmad
akhairul@uthm.edu.my

[1] Microelectronic and Nanotechnology-Shamsuddin Research Centre (MiNT-SRC), Faculty of Electrical and Electronic Engineering, Universiti Tun Hussein Onn Malaysia, 86400 Parit Raja, Batu Pahat, Johor, Malaysia

[2] Nanotechnology Research Centre, Department of Physics, Faculty of Science and Mathematics, Universiti Pendidikan Sultan Idris, 35900 Tanjung Malim, Perak, Malaysia

[3] Nano-ElecTronic Centre, Faculty of Electrical Engineering, UiTM, 40450 Shah Alam, Selangor, Malaysia

[4] Department of Engineering, Graduate School of Integrated Science and Technology, Shizuoka University, Hamamatsu, Shizuoka 432-8011, Japan

1 Introduction

Titanium dioxide, also known as titanium oxide or titania, is found in three natural crystalline phases namely, anatase, rutile and brookite. Titanium dioxide has a melting point of 1825 °C which implies strong bond, high thermal stability and chemical resistance [1]. Both rutile and anatase titanium dioxide have a tetragonal structure but with different space groups. Rutile has a space group of $P4_2/mnm$ with two titanium dioxide formula units in one cell, while anatase belongs to group $I4_1/amd$ with four titanium dioxide formula units in one cell [2]. Active crystallite phases for titanium dioxide are rutile and anatase although brookite is occasionally used in chemical reactions [3, 4].

Unique physical and chemical properties of polycrystalline titanium dioxide has made it suitable for several important industrial applications including photocatalysis [5], photovoltaics [6] and photosensors [7]. It is an important material because of its functional properties. For example, under certain conditions, it can absorb ultraviolet (UV) light [8] and is transparent under visible light spectrum [9]. Generally, the rutile phase titanium dioxide is obtained from the calcination process of anatase titanium dioxide. The calcination process is normally conducted at a temperature range of 400–1000 °C, though the actual transformation normally occurs at around 800–850 °C [10].

Raman spectroscopy is commonly used to investigate titanium dioxide structural properties, where changes in diameter of the particles being one of the parameters that will induce change in peak intensity and broadening of Raman bands. Raman spectroscopy help us understand the role of strain energy, quantization effect and formation of stable phase of TiO_2 nanoparticles [11]. In the present work, r-TNRs/r-TNFs were synthesized by hydrothermal

Published online: 09 April 2016

method for various reaction times. An investigation was conducted to see the effect of various reaction times on the structural property and surface morphology of titanium dioxide and the Raman spectra. These films are suitable in various applications such as UV light sensors and solar cells.

2 Experimental

Rutile-phased titanium dioxide nanorods (r-TNRs) and rutile-phased titanium dioxide nanoflowers (r-TNFs) were synthesized from a chemical solution using the hydrothermal process. The chemical solution was prepared by dissolving 120 mL of concentrated hydrochloric acid (HCl) (36.5–38 %) in 120 mL of deionized (DI) water. The mixture was vigorously stirred for 5 min before 6 mL of titanium butoxide (TBOT) was added drop wise using a capillary tube. After stirring for nearly 20 min, the solution was placed into steel made autoclave with Teflon made liner (300 mL) for hydrothermal process in which the FTO glass substrates were placed with the conducting FTO surface facing upwards. The process was performed at 150 °C for reaction times 2, 3, 4, 5, 6, 7 and 8 h. After that, the autoclave was taken out from the oven and was let to cool to room temperature. The prepared samples were rinsed with DI water and left to dry at room temperature. The morphology and thickness of TiO_2 nanorods were characterized by using a field emission scanning electron microscope (FESEM) JEOL JSM-7600F model operated at 15 kV. Chemical composition of the samples were characterized using an energy dispersive X-ray spectroscope (EDS Oxford Instrument Inc.) attached to the FESEM. The crystal structure and crystallite size are defined by an X-ray diffractometer (XRD) PANalytical X-Pert^3 Powder model. The scan axis used were 2θ with range of 20°–60° and the type of slit used were fixed divergence slit. Finally, Raman spectra were obtained using a Micro-Raman Spectroscope (Renishaw InVia microRaman System) operated with 514 nm wavelength of argon (Ar^+) laser.

3 Results and discussion

3.1 Surface morphology and chemical composition

Chemical composition of the samples is presented in Table 1. From Table 1, it can be seen that the weight percentage of Ti increased as reaction time increased. Surface morphologies of r-TNRs array prepared at different hydrothermal reaction times are shown in Fig. 1a–g. Figure 1a shows the surface morphology of the sample prepared at 2 h reaction time. The FESEM image corresponds to FTO structures and neither nanorods nor TiO_2 nanoparticles were detected [12]. This can also be confirmed with the EDS data as shown in Table 1. Growth of r-TNRs was detected as the reaction time was increased to 3, 4, 5, 6, 7 and 8 h, as shown in Fig. 1b, c, d, e, f, and g, respectively. FESEM image of the sample prepared at 3 h reaction time, as shown in Fig. 1b, shows a surface morphology of r-TNRs with thickness of 0.19 μm. The rods are in slanting position with big gaps between each other. Figure 1c, d show highly oriented tetragonal r-TNRs with thickness of 0.54 and 1.41 μm, respectively. The gaps between the rods and the thickness of the rods for sample prepared at 5 h reaction time were slightly bigger than the sample prepared at 4 h reaction time. As reaction time increased from 5 to 8 h, the r-TNRs formed were bigger in diameter. FESEM image of the sample prepared at 6 h reaction time, as shown in Fig. 1e, shows an increase in thickness and diameter of r-TNRs, thus eliminating the gaps between the nanorods. FESEM image of the sample prepared at 7 h reaction time, as shown in Fig. 1f, shows that the thickness of r-TNRs has greatly enhanced to 4.13 μm with no gaps or boundaries formed between the rods. Meanwhile, the thickness of r-TNFs for the sample prepared at 8 h reaction time, as shown in Fig. 1g, has slightly decreased to 3.19 μm due to the abundance of r-TNFs growing on top of it which also hindered the growth of nanorods. With short reaction time, the obtained nanorods were not as aligned as the samples obtained with longer reaction times.

In this study, the outcome also consisted of nanoflowers (TNFs). TNFs grew in samples prepared at 3, 4, 5, 6, 7 and

Table 1 EDS data for samples prepared at 2, 3, 4, 5, 6, 7 and 8 h reaction times

Reaction time (h)	Element W = weight % A = atomic %		
	Sn	O	Ti
2	W = 60.80 A = 17.29	W = 39.20 A = 82.71	–
3	W = 56.95 A = 15.84	W = 39.66 A = 81.83	W = 3.39 A = 2.33
4	W = 33.61 A = 8.12	W = 43.67 A = 78.28	W = 22.72 A = 13.60
5	W = 2.96 A = 0.59	W = 52.81 A = 77.68	W = 44.23 A = 21.73
6	–	W = 48.85 A = 74.09	W = 51.15 A = 25.91
7	–	W = 46.95 A = 72.60	W = 53.05 A = 27.40
8	–	W = 44.73 A = 70.79	W = 55.27 A = 29.21

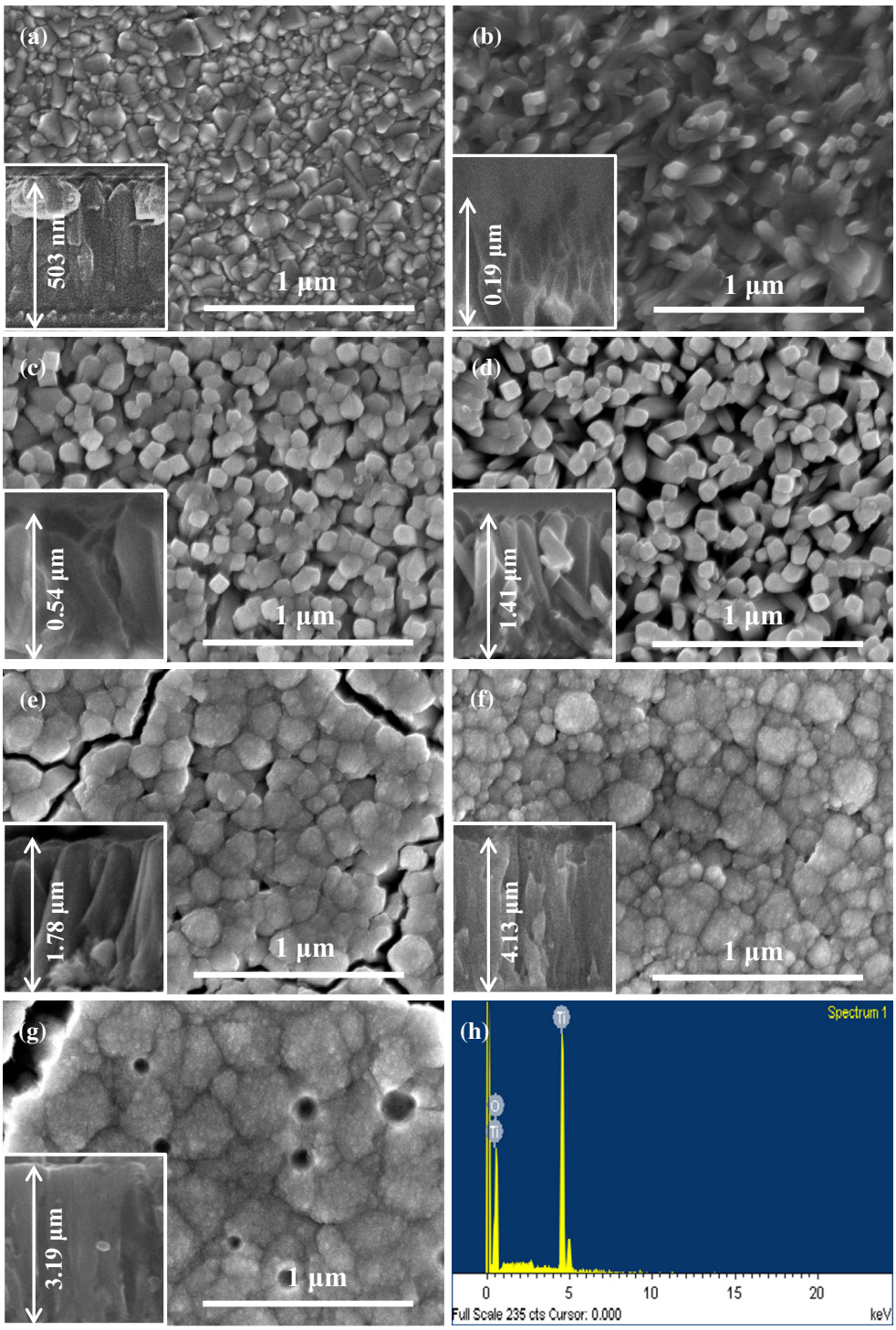

Fig. 1 Surface morphology images of TiO_2 nanorods array for **a** 2, **b** 3, **c** 4, **d** 5, **e** 6, **f** 7, and **g** 8 h hydrothermal synthesis time with 25 k magnification. **h** The EDS spectra for 6 h synthesis time. The *insets* are the corresponding cross-sectional views of each sample

8 h reaction time, as shown in Fig. 2a, b, c, d, e, and f, respectively. The nucleation process of TNFs is interpreted to have begun by deposition on the tip of the r-TNRs, as shown in FESEM image of the sample treated for 3 h, as shown in Fig. 2a. As reaction time increased to 4 h, the flowers have started to grow, as shown in Fig. 2b. At 5 h reaction time, the flowers became longer and thinner and eventually thicker at 6 h reaction time shown in Fig. 2c and d, respectively. The flowers reached their stable state at 7 h reaction time. As the time increased, the flowers

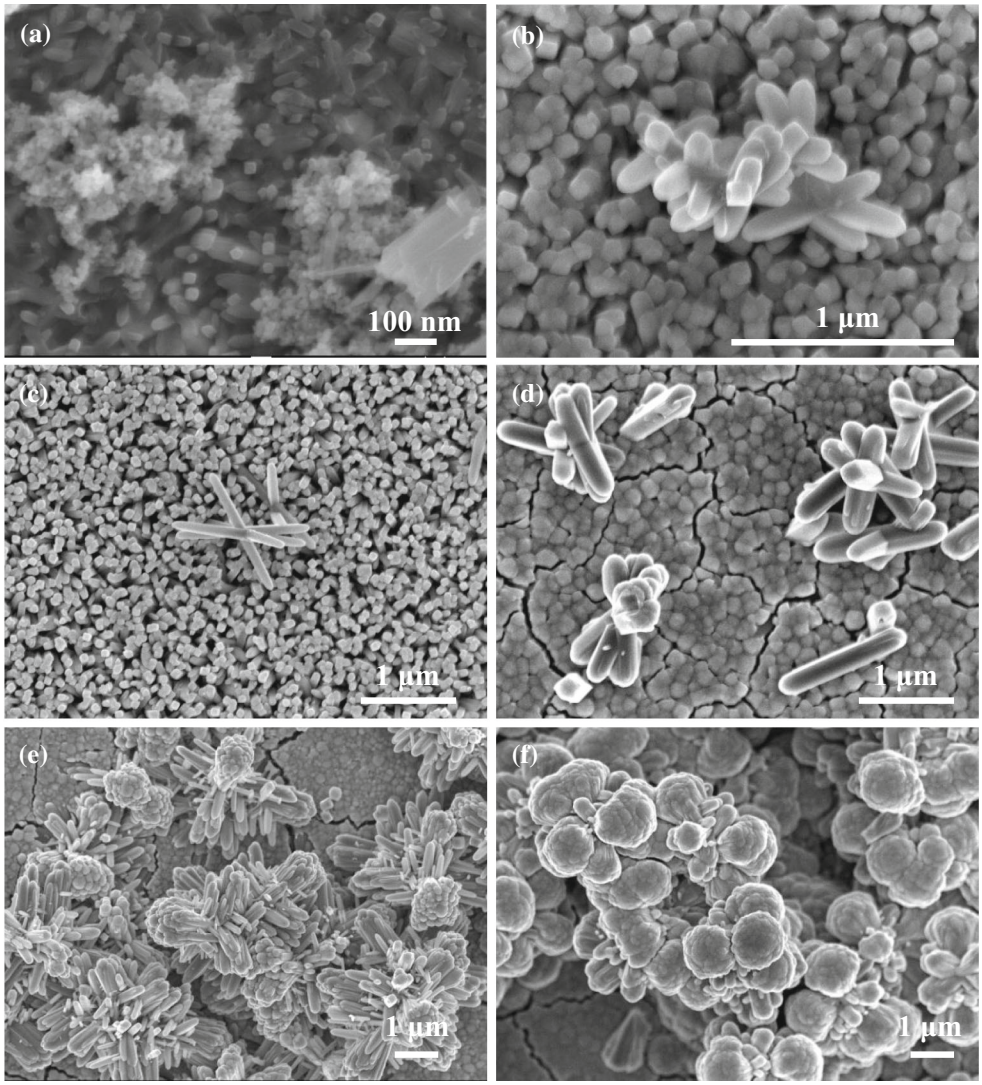

Fig. 2 Morphologies image of TiO2 nanoflowers for **a** 3, **b** 4, **c** 5, **d** 6, **e** 7, and **f** 8 h hydrothermal synthesis time with different magnification

agglomerated to become larger in size, as a result cauliflower-like nanoflowers can be seen in the sample treated for 8 h in Fig. 2f. The growth mechanism is illustrated in Fig. 3.

3.2 X-ray diffraction

XRD spectra of TiO_2 samples prepared at various reaction times were shown in Fig. 4. Typical XRD pattern of the samples synthesized at various reaction times are shown in Fig. 4a, b, c, d, e, f, g. As shown in Fig. 4a, the XRD pattern of the TiO_2 sample prepared at 2 h well matched the XRD diffraction of a blank FTO with peaks at 26°, 34°, 37°, 51° and 55°. This is confirmed with the FESEM image of the sample prepared at 2 h which showed only FTO morphology. The peaks for samples prepared at 3, 4 and 5 h reaction times as shown in Fig. 4b, c, and d, respectively, were a mixed between FTO phase and rutile phase. The sample prepared at 3 h reaction time has only 1 peak of rutile, which corresponds to plane [101], showing that r-TNRs have started to grow. For the sample prepared at 4 h, as shown in Fig. 4c, there are three out of seven peaks of rutile phase corresponding to plane [101], [111], and [211]. Starting from the 4th hour, the intensity of FTO peaks have decreased. Meanwhile, for the sample prepared at 5 h, Fig. 4d exhibited three FTO peaks with very low intensity and three same rutile peaks as the sample prepared at 4 h. This can be attributed to the thickness of r-TNRs/TNFs that has increased with increasing reaction time. Initially, there is no peak produced at 27.4° for samples prepared at 2, 3, 4, and 5 h reaction time. As the time increased, it can be seen that an additional peak formed, as shown in Fig. 4e–g. This indicates that an additional nanostructure grew in the thin film sample which

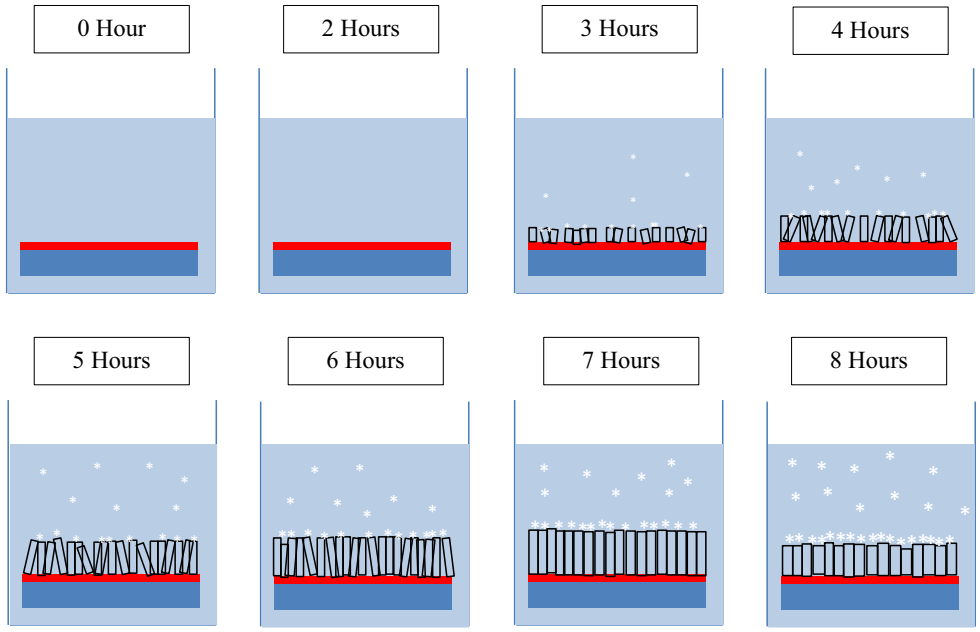

Fig. 3 Growth mechanism of r-TNR/r-TNF for each reaction time

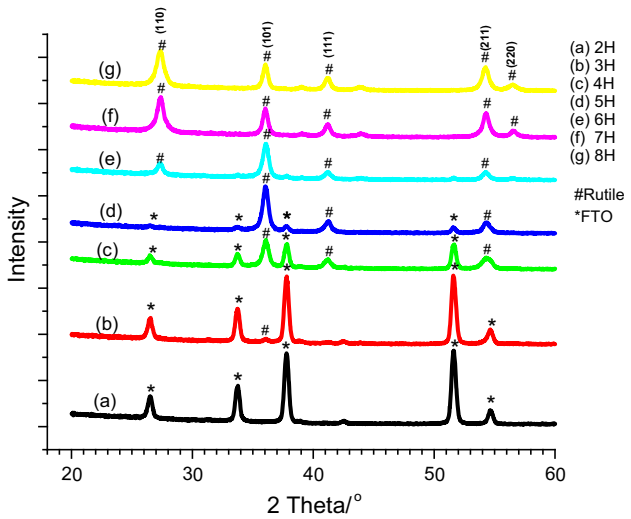

Fig. 4 X-ray diffraction pattern of r-TNR/r-TNF with different hydrothermal synthesis time

is the TNFs. The additional peak at 27.4° represents plane [110]. Peaks for the sample prepared at 6 h, as shown in Fig. 4e all corresponds to rutile peaks. For the XRD patterns of the sample prepared at 7 and 8 h, as shown in Fig. 4f, g, there is one additional rutile peak that can be seen. The peak located at 56.6° representing plane [211]. This shows that by increasing reaction time, the sample will have a stronger crystallinity. From the full-width half-maximum (FWHM) of the samples, the entire peaks observed gave either a strong and sharp diffraction, or a weak and sharp diffraction. There is no broad peak detected thus showing that the entire samples possess good crystallinity.

From the XRD data, the crystallite size of the samples can be obtained by using Scherrer's formula [12]:

$$D = \frac{k\lambda}{\beta cos\theta} \quad (1)$$

where, D is the crystallite size, k is the Scherrer coefficient, λ is the CuKα radiation wavelength, β is the FWHM of the diffraction peak and θ is the diffraction angle. Table 2 shows the value of crystallite size obtained for each sample. The crystallite size does not show a significant change with increasing reaction time. The crystallite size may change if various temperatures are applied during the reaction process [7, 13].

Table 2 Crystallite size for each sample calculated from XRD data

Reaction time (h)	FWHM	Crystallite size (Å)
2	0.3542	4.91
3	0.3149	5.52
4	0.2755	6.31
5	0.3149	5.52
6	0.3936	4.42
7	0.4330	4.02
8	0.4330	4.02

3.3 Micro-Raman spectroscopy

Raman spectra for blank FTO as a controlled sample were shown in Fig. 5. The Raman spectra of TiO_2 thin films prepared by hydrothermal treatment for 2–8 h are shown in Fig. 6. The peak positions produced for the sample prepared at 2 h reaction time shows the same peaks as controlled FTO at 555, and 1084 cm^{-1}. For the sample prepared at 3 h hydrothermal treatment, there are mixed peaks of FTO and r-TNRs/r-TNFs; at 122, 242, 441 and 622 cm^{-1} for rutile phase and 555 and 1084 cm^{-1} for FTO. Beginning from 4 h and above, all peaks are the Raman shifts of rutile crystal [14–16]. The samples exhibit dominant peaks at 118 cm^{-1} (B_{1g}), 449 cm^{-1}(E_g), and 609 cm^{-1} (A_{1g}), which are assigned to the three Raman active modes of rutile single crystal expressed as $A_{1g} + B_{1g} + E_g$. For rutile phase, two prominent maxima at 445 and 609 cm^{-1} [17] are comparable with the entire peaks produced. In addition, there are second-order scatterings featured at 241 cm^{-1} (E_g) peak due to the multiple-phonon scattering process and 690 cm^{-1} broad peak caused by small r-TNRs/TNFs formed, which is also considered as a characteristic of rutile type TiO_2 [18, 19]. The weak and broad band at 241 cm^{-1} is likely due to phonon confinement effect where the decrease in particles dimension to the nanometres scale caused a wave number blue shift and in this case, broadening of Raman peaks. Raman spectra of this sample are in E_g and A_{1g} mode, as well as the second order effect as the major feature. Meanwhile, the B_{1g} mode is either weak or absent. The intensity of the Raman peaks is enhanced at 5 h reaction time while there are no significant changes at 6, 7, and 8 h reaction time. These changes can be attributed to the crystallite sizes of the samples [20]. But from XRD, we found that the crystallite size have no significant changes with varying reaction time and the Raman spectra behaviour also could not be explained using the phonon confinement model [21] as the observed peak does not show any effect of crystallite size. This abnormal behaviour of the Raman bands may be caused by the shape and morphology distribution of various TiO_2 structures, which affect the peak position and line width of TiO_2 Raman bands [11]. From FESEM image, it can be seen that the TiO_2 thin film for 5 h reaction was mostly nanorods which contribute to the c-plane miller indices on XRD. Meanwhile for 6, 7, and 8 h reaction time, there were lots of nanoflowers growths on top of the nanorods thin film making the intensity for c-plane to decrease. This explains the sudden decrease of Raman intensity at 118 cm^{-1} for 6, 7, and 8 h reaction time. Figure 7 shows normalized Raman spectra for 2–4 h.

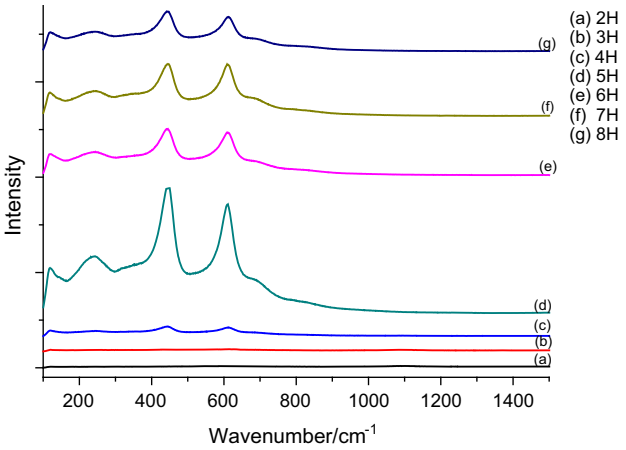

Fig. 6 Micro-Raman spectroscopy of nanorods array TiO_2 with different hydrothermal synthesis

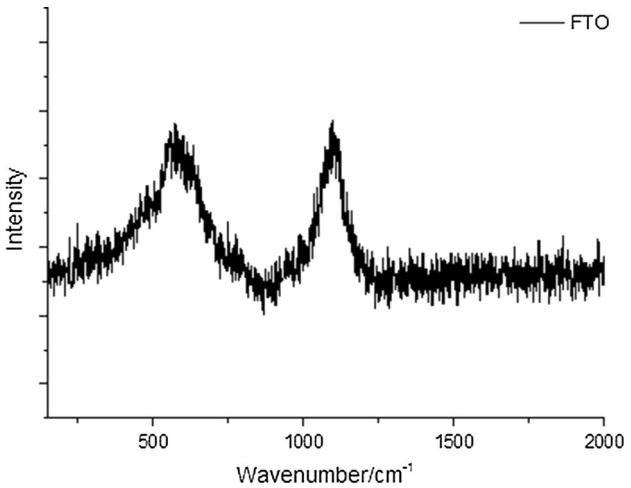

Fig. 5 Micro-Raman spectroscopy for blank FTO as control for this experiment

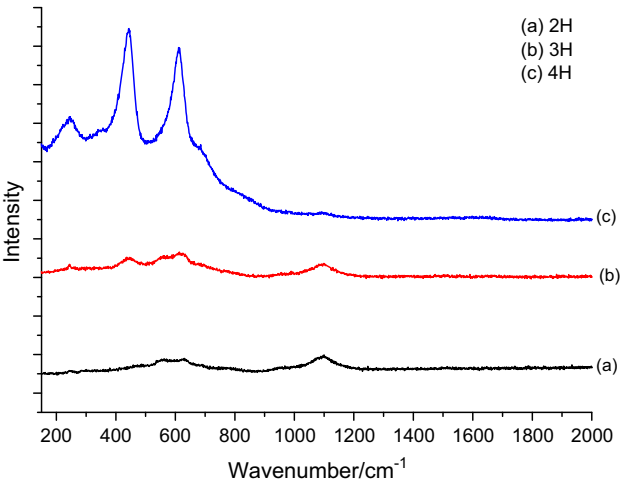

Fig. 7 Normalized micro-Raman spectroscopy of nanorods array TiO_2 for *a* 2H, *b* 3H, and *c* 4H hydrothermal time

4 Conclusion

In this study, we prepared r-TNRs directly on FTO substrate with r-TNFs grown on top of the r-TNRs using a one-step hydrothermal process. The reaction time was varied from 2 to 8 h. FESEM images of the resulting structure show that the thickness of the nanorods increased as hydrothermal reaction time increased and eventually decreased at 8 h reaction time due to the hindrance by abundant r-TNFs. All of the fabricated samples have the crystalline structure in rutile phase according to the XRD pattern except for the sample prepared at 2 h reaction that shows only FTO peaks. Raman spectra of the samples show abnormal behaviour of the intensity which changes insignificantly, in addition to shifting of its bands with increasing reaction time. This behaviour is due to shape, size and morphology distribution of the r-TNRs/r-TNFs.

Acknowledgments The authors would like to thank the Ministry of Education (MOE) Malaysia (Vot 1213), Microelectronic and Nanotechnology-Shamsuddin Research Centre (MiNT-SRC) and Universiti Tun Hussein Onn Malaysia (UTHM) for financial support using Vot U331.

References

1. I. Lukačević, S.K. Gupta, P.K. Jha, D. Kirin, Lattice dynamics and Raman spectrum of rutile TiO_2: the role of soft phonon modes in pressure induced phase transition. Mater. Chem. Phys. **137**(1), 282–289 (2012)
2. Y. Wang, L. Zhang, K. Deng, X. Chen, Z. Zou, Low temperature synthesis and photocatalytic activity of rutile TiO_2 nanorod superstructures. J. Phys. Chem. C **111**, 2709–2714 (2007)
3. Y. Ohno, K. Tomita, Y. Komatsubara, T. Taniguchi, K. Katsumata et al., Pseudo-cube shaped brookite (TiO_2) nanocrystals synthesized by an oleate-modified hydrothermal growth method. Cryst. Growth Des. **11**(11), 4831–4836 (2015)
4. M. Landmann, E. Rauls, W.G. Schmidt, The electronic structure and optical response of rutile, anatase and brookite TiO_2. J. Phys.: Condens. Matter **24**(19), 195503 (2012)
5. A.L. Linsebigler, A.L. Linsebigler, J.T. Yates Jr, G. Lu, G. Lu, J.T. Yates, Photocatalysis on TiO_2 surfaces: principles, mechanisms, and selected results. Chem. Rev. **95**(3), 735–758 (1995)
6. J. Xiong, B. Yang, J. Yuan, L. Fan, X. Hu, H. Xie, L. Lyu, R. Cui, Y. Zou, C. Zhou, D. Niu, Y. Gao, J. Yang, Efficient organic photovoltaics using solution-processed, annealing-free TiO_2 nanocrystalline particles as an interface modification layer. Org. Electron. **17**, 253–261 (2015)
7. M. Okuya, K. Shiozaki, N. Horikawa, T. Kosugi, G.R.A. Kumara, J.Á. Madarász, S. Kaneko, G. Pokol, Porous TiO_2 thin films prepared by spray pyrolysis deposition (SPD) technique and their application to UV sensors. Solid State Ionics **172**(1–4), 527–531 (2004)
8. Abdul Qader Dawood Faisal, Synthesis and characteristic study of TiO_2 nanowires and nanoflowers on FTO/glass and glass substrates via hydrothermal method. J. Mater. Sci.: Mater. Electron. **26**, 317–321 (2015)
9. H. Yang, S. Zhu, N. Pan, Studying the mechanisms of titanium dioxide as ultraviolet-blocking additive for films and fabrics by an improved scheme. J. Appl. Polym. Sci. **92**(5), 3201–3210 (2004)
10. B. Grzmil, B. Kic, M. Rabe, Inhibition of the anatase—rutile phase transformation with K_2O, P_2O_5, Li_2O. Chem. Pap. **58**, 410–414 (2004)
11. M.C. Mathpal, A.K. Tripathi, M.K. Singh, S.P. Gairola, S.N. Pandey, A. Agarwal, Effect of annealing temperature on Raman spectra of TiO2 nanoparticles. Chem. Phys. Lett. **555**, 182–186 (2013)
12. E.V.A. Premalal, N. Dematage, S. Kaneko, A. Konno, Preparation of high quality spray-deposited fluorine-doped tin oxide thin films using dilute di(n-butyl)tin(iv) diacetate precursor solutions. Thin Solid Films **520**(22), 6813–6817 (2012)
13. L. Kernazhitsky, V. Shymanovska, T. Gavrilko, V. Naumov, L. Fedorenko, V. Kshnyakin, J. Baran, Room temperature photoluminescence of anatase and rutile TiO_2 powders. J. Lumin. **146**, 199–204 (2014)
14. H.L. Ma, J.Y. Yang, Y. Dai, Y.B. Zhang, B. Lu, G.H. Ma, Raman study of phase transformation of TiO_2 rutile single crystal irradiated by infrared femtosecond laser. Appl. Surf. Sci. **253**(18), 7497–7500 (2007)
15. P. Liu, W. Cai, M. Fang, Z. Li, H. Zeng, J. Hu, X. Luo, W. Jing, Room temperature synthesized rutile TiO(2) nanoparticles induced by laser ablation in liquid and their photocatalytic activity. Nanotechnology **20**(28), 285707 (2009)
16. H.W. Kim, H.S. Kim, H.G. Na, J.C. Yang, D.Y. Kim, Growth, structural, Raman, and photoluminescence properties of rutile TiO_2 nanowires synthesized by the simple thermal treatment. J. Alloys Compd. **504**(1), 217–223 (2010)
17. S.S. Mali, C.A. Betty, P.N. Bhosale, R.S. Devan, Y.-R. Ma, S.S. Kolekar, P.S. Patil, Hydrothermal synthesis of rutile TiO_2 nanoflowers using brønsted acidic ionic liquid [BAIL]: synthesis, characterization and growth mechanism. CrystEngComm **14**(6), 1920 (2012)
18. S. Sugapriya, R. Sriram, S. Lakshmi, Effect of annealing on TiO_2 nanoparticles. Optik **124**(21), 4971–4975 (2013)
19. M. Gotić, M. Ivanda, S. Popović, S. Musić, A. Sekulić, A. Turković, K. Furić, Raman investigation of nanosized TiO_2. J. Raman Spectrosc. **28**(7), 555–558 (1997)
20. X. Xue, W. Ji, Z. Mao, H. Mao, Y. Wang, X. Wang, W. Ruan, B. Zhao, J.R. Lombardi, Raman investigation of nanosized TiO_2: effect of crystallite size and quantum confinement. J. Phys. Chem. C **116**(15), 8792–8797 (2012)
21. S.Y.D.J.R. Balaji, Phonon confinement studies in nanocrystalline anatase–TiO_2 thin films by micro Raman spectroscopy. J. Raman Spectrosc. **37**, 1416–1422 (2006)